

Ni-Catalyzed Reductive Coupling of Acetals with Anhydrides and Vinyl Triflates via Single-Electron C–O Activation

Eunbi Kim,[†] Meredith A. Borden,[†] Junha Hwang, Abigail G. Doyle,* and Sun Dongbang*



Cite This: *Org. Lett.* 2025, 27, 9454–9459



Read Online

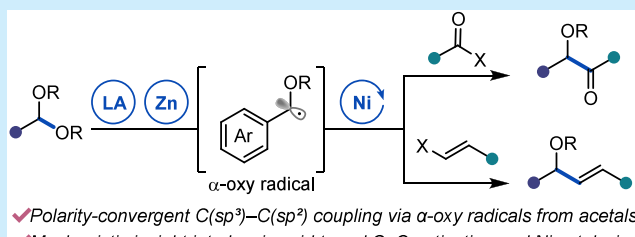
ACCESS |

Metrics & More

Article Recommendations

Supporting Information

ABSTRACT: We report a Ni-catalyzed reductive cross-coupling of benzaldehyde-derived acetals with anhydrides or vinyl triflates, enabling modular access to α -substituted ethers. Lewis acid/Zn-mediated activation generates α -oxy radicals for selective $C(sp^3)$ – $C(sp^2)$ bond formation via Ni catalysis. This polarity-convergent method unifies ether-variants of benzoin condensation and classical NHK reactions under one reductive platform. Broad scope is demonstrated, and tuning the Lewis acid extends reactivity to dialkyl acetals. Stoichiometric, organometallic, and spectroscopic studies support the reaction mechanism.



Aldehydes are essential building blocks in organic synthesis. Numerous transformations, such as the Grignard and Nozaki-Hiyama-Kishi (NHK) reactions, leverage the innate polarity of the carbonyl group for C–C bond formation with organometallics.¹ Alternatively, umpolung reactivity, such as in the benzoin condensation, reverses the normal carbonyl polarity to enable C–C bond formation with another aldehyde, accessing α -hydroxy ketones (Scheme 1A).² However, due to their high reactivity, aldehydes generally cannot be carried through multistep synthetic sequences. In such cases, acetals are often used as a protecting group to mask the aldehyde reactivity and easily removed for downstream transformations (Scheme 1B, top).³

Although acetals are common protecting groups for aldehydes, direct C–O activation for C–C bond formation remains relatively underexplored. If such potential was unlocked, employing acetals as building blocks for direct C–C bond formation could provide a step-economical approach to accessing α -substituted ethers from aldehydes by obviating the steps of deprotection and alkylation (Scheme 1B, bottom). α -Substituted ethers are pervasive structural motifs found in biologically active compounds, rendering them valuable synthetic targets.⁴

Several methods have been reported to enable reductive C–O bond activation and C–C bond formation. The Hatano group first reported the reductive C–O bond cleavage of acetals, using a Lewis acid to activate the acetal and Zn as the reductant for single electron transfer (SET); upon radical recombination, the radical dimer was generated (Scheme 1C, a).^{5a} Expanding from homocoupling to cross-coupling, the Doyle group developed a Ni-catalyzed cross-electrophile coupling between benzylic acetals and aryl iodides under reductive conditions (Scheme 1C, b).^{5b} Analogously, use of a Lewis acid and Zn provided an α -oxy carbon radical,^{5a} which

could be trapped by a Ni(II) species derived from oxidative addition of Ni with the aryl iodide. Based on this report, the Wang group reported a method for the synthesis of *gem*-difluoroalkenes by merging C–F and C–O bond cleavage from Ni(I) under reductive conditions (Scheme 1C, c).^{5c} In 2019, Dixon showcased that ketyl radicals, generated by an Ir-photocatalyst and Hantzsch ester as the reductant, undergo radical addition to electron-deficient alkenes (Scheme 1C, d).^{5d} These examples demonstrate the potential of acetals as radical precursors for C–C bond formation, but transition-metal-catalyzed methods and mechanistic studies enabling distinct C–C bond-forming transformations remain largely underexplored.⁶

Herein, we report a strategy for accessing α -substituted ethers via $C(sp^3)$ – $C(sp^2)$ bond formation by leveraging the intermediacy of α -oxy radicals generated from acetals by SET.⁷ Interfacing these radicals with a Ni catalyst and anhydrides or vinyl triflates delivers a library of ethereal products (Scheme 1D). Using anhydrides as coupling partners provides complementary reactivity to the classical cross-benzoin condensation, which often suffers from poor chemoselectivity due to the use of two aldehydes as coupling partners.⁸ Reaction with vinyl triflates offers access to ether derivatives of classical NHK reaction products without requiring toxic chromium reductant.^{1b,9} This methodology enables a single set of

Received: July 9, 2025

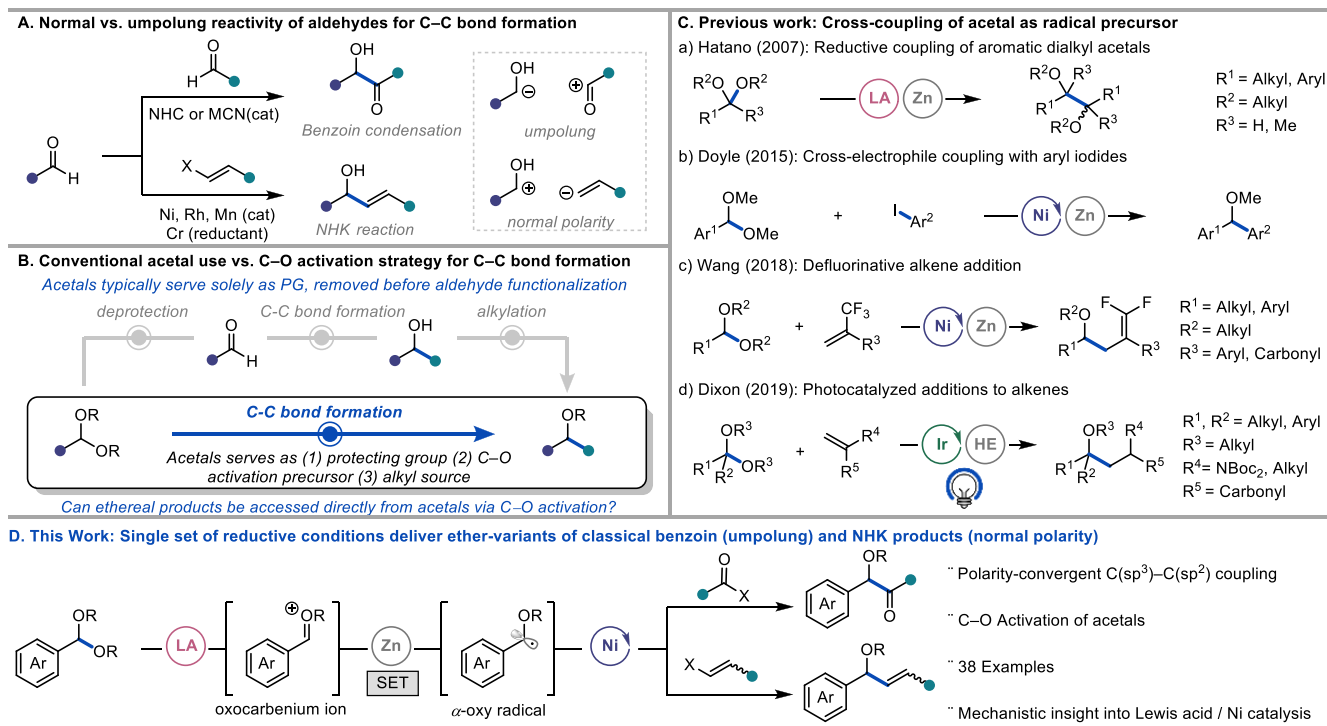
Revised: August 8, 2025

Accepted: August 12, 2025

Published: August 18, 2025



Scheme 1. C–C Bond Formation from Aldehyde and Acets



conditions where traditionally a distinct polarity mode would have been required.

With these goals in mind, we commenced our investigation by using benzaldehyde dimethyl acetal **1a** and propionic anhydride **2a** as model substrates (Table 1, see SI II-A).¹⁰ Systematic evaluation of the reaction parameters revealed that aldehyde **3aa** and dimer **3ab** were the major side products. Under optimal conditions, 10 mol% NiCl₂·DME with tridentate ligand bpp(2,6-bis(*N*-pyrazolyl)pyridine) gave the desired product **3a** in 96% yield (Table 1, entry 1). Omission of any components resulted in no reactivity (entry 2–5). Reducing the equivalents of **2a** led to the increase in formation of **3ab** (entry 6). Ligand screening identified bpp as optimal, while common Ni ligands (e.g., terpy, biox, bpy, phen) were less effective and promoted **3ab** formation (entry 7–10, for more detailed optimization see SI II-C).

With the optimized conditions in hand, we evaluated the anhydride scope (Table 2A). α - and β -branched acyl coupling partners (**3b–3d**) showed high conversion to the desired products, while an ester-containing anhydride provided **3e** in 63% yield. Benzoic anhydride was also effective (**3f**), albeit in a lower yield, with dimer **3ab** comprising most of the remaining mass balance.

We also varied the arene of the dimethyl acetal (Table 2B). Acetals bearing extended conjugation systems such as naphthyl (**3g**) or electron-neutral to -rich arenes bearing *para*-fluoro (**3h**) and *para*-*t*-butyl (**3i**) afforded good yields. *meta*-Substituted arenes with *meta*-vinyl (**3j**) or methoxy (**3k**) groups also gave high yields. Acetals with electron-deficient arenes exhibited excellent yields but required more TMSCl and heat (**3l–3n**). Cyclic acetals such as dioxolane-, phthalan-, and isochroman-derived acetals also gave high yields to the desired product (**3o–3q**). For dioxolane-derived acetal (**1q**), the immediate product exists as an equilibrium between the 1° alcohol and the cyclic 6-membered dioxanol.¹¹ Therefore, we

Table 1. Deoptimization of Dialkyl Ether Formation with Benzaldehyde Dimethyl Acetal and Propionic Anhydride^a

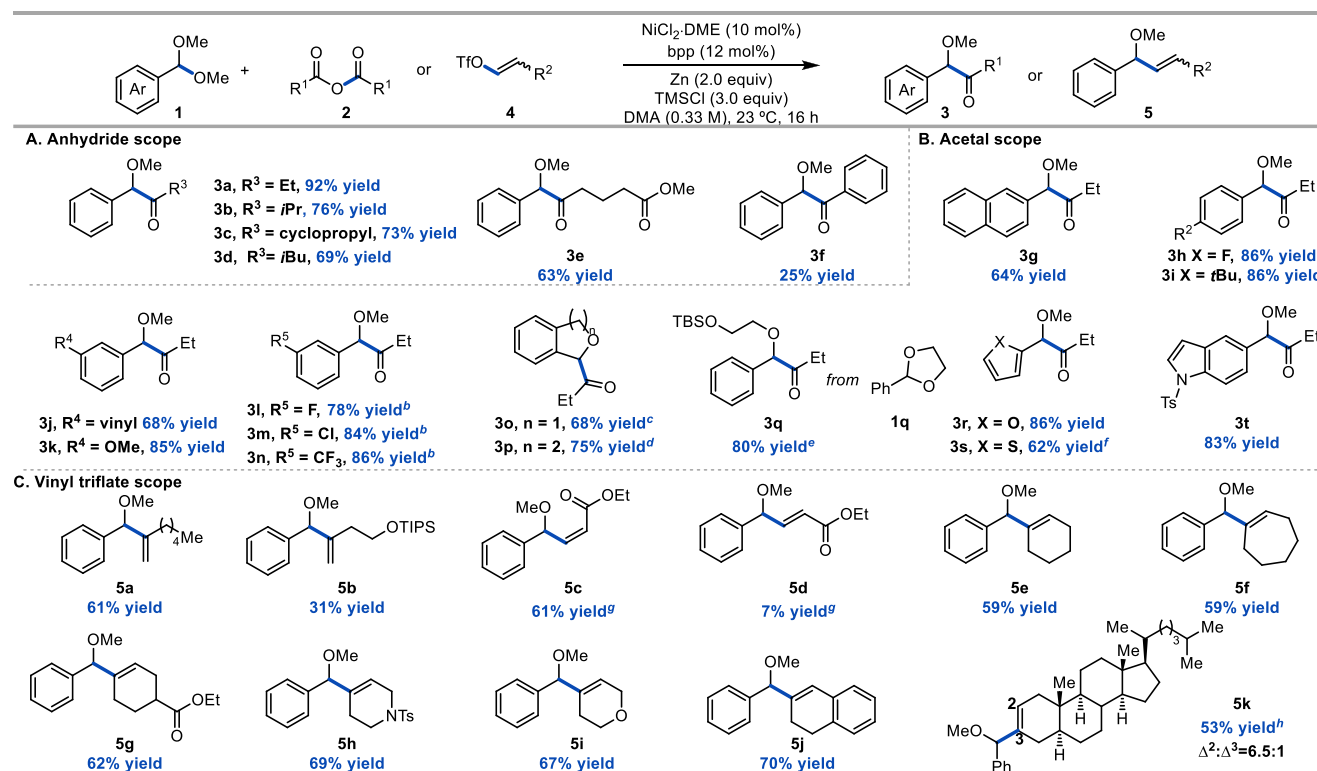
Yield (%)^a

Entry	Deviation from standard conditions	Yield (%) ^a		
		3a	1a	3aa
1	none	96	0	0
2	no bpp	0	0	0
3	no Ni, no bpp	0	0	0
4	no Zn	0	36	38
5	no TMSCl	0	78	0
6	1.0 equiv of anhydride	47	0	0
7	terpy instead of bpp	9	0	0
8	Bn-biox instead of bpp	19	75	0
9	bpy instead of bpp	50	0	0
10	phen instead of bpp	19	0	0

bpp = 2,6-bis(*N*-pyrazolyl)pyridine, **terpy** = 2,2':6',2"-terpyridine, **Bn-biox** = benzyl bisbioxazoline, **bpy** = 2,2'-bipyridine, **phen** = 1,10-phenanthroline

^aReactions performed on 0.10 mmol scale. Yields were determined by ¹H NMR using 1,3,5-trimethoxybenzene as the external standard. bpp = 2,6-bis(*N*-pyrazolyl)pyridine, terpy = 2,2':6',2"-terpyridine, Bn-biox = benzyl bisbioxazoline, bpy = 2,2'-bipyridine, phen = 1,10-phenanthroline.

trapped the resulting 1° alcohol with a TBS group, affording an 80% yield over two steps (**3q**). Acetals bearing medicinally

Table 2. Benzaldehyde Dimethyl Acetal and Anhydride Scope^a

^a Isolated yield from 0.50 mmol using anhydrides (2.0 equiv). Average of two runs. ^b TMSCl (5.0 equiv) at 50 °C. ^c From 1,3-dihydro-1-methoxyisobenzofuran. ^d From 1-methoxyisochroman; BF₃·OEt₂ (3.0 equiv) instead of TMSCl. ^e Yield from 2-phenyl-1,3-dioxolane followed by TBS protection; 2-step yield. ^f Propionic anhydride (5.0 equiv) used. ^g Using vinyl iodide instead of vinyl triflate. ^h Performed on a 0.30 mmol scale using an 8:1 mixture of vinyl triflates derived from 5 α -cholestane-3-one.

relevant, electron-rich heterocycles, such as furan, thiophene, and indole, underwent coupling in moderate to high yield (3r–3t).

We next evaluated vinyl triflates as coupling partners, offering a complementary C–C bond-forming strategy to the classical NHK reaction (Table 2C). α -Substituted vinyl triflates reacted efficiently to give **5a** in a good yield. A silyl-protected alcohol-bearing triflate provided **5b** in a 31% yield. While Z-iodoacrylate gave **5c** in high yield, *E*-idoacrylate gave poor conversion to **5d**. Six- and seven-membered cyclic vinyl triflates furnished **5e**–**5g** in moderate yields. Heterocyclic triflates including piperidine and pyran groups afforded the product in good yields, showing excellent functional group tolerance (**5h**, **5i**). Conjugated vinyl triflates also coupled efficiently (**5j**). Notably, a cholesterol-derived triflate delivered **5k** in 53% yield, highlighting the potential for steroid derivatization.¹²

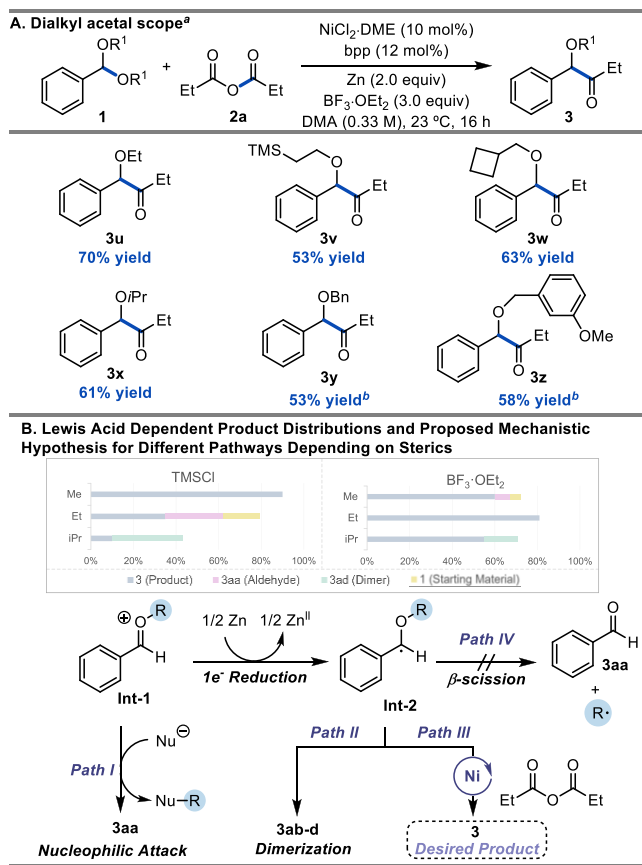
Next, we examined benzaldehyde dialkyl acetals beyond dimethyl acetals but observed decreasing yields with increasing alkyl steric bulk—35% for diethyl (**1u**) and 10% for diisopropyl acetal (**1x**) (Table 3, see SI V-A). Further optimization with **1u** revealed that the choice of Lewis acid was critical, with BF₃·OEt₂ giving the highest yield (Table 3A). Using BF₃·OEt₂, benzaldehyde dialkyl acetals containing unactivated linear alkyl chains, such as ethyl (**3u**), trimethylsilyl (**3v**), and cyclobutane ethyl (**3w**) gave high yields. Notably, even the sterically hindered diisopropyl acetal provided **3x** in 61% yield, highlighting the utility of this method for challenging C–O bond activation systems.⁵

Benzaldehyde dibenzyl acetals were also competent for this reaction (**3y**, **3z**).

During the reoptimization process, we observed that benzaldehyde dialkyl acetals with different sterics, when combined with various Lewis acids, produced distinct side products. With TMSCl, **1a** generated negligible side products, whereas reactions with **1u** produced the benzaldehyde **3aa**, and those with **1x** generated the dimerized **3ad** (Table 3B). When TMSCl was replaced with BF₃·OEt₂, a smaller and more Lewis acidic additive, the yield with **1a** decreased, accompanied by increased benzaldehyde **3aa**. In contrast, the yield with **1u** significantly improved with minimal side product formation. Reaction of **1x** also showed improved yield, though with a higher ratio of dimerized **3ad**.

Based on these observations, we postulate that because **1a** is unhindered, it easily forms an α -oxy radical with TMSCl but is too reactive and susceptible to decomposition with the stronger Lewis acid BF₃·OEt₂. In contrast, the more hindered **1u** and **1x** require a more strongly activated Lewis acid such as BF₃·OEt₂ to access the acetal oxygen for oxocarbenium ion generation. The different side products arising from **1u** vs **1x** likely arise from distinct pathways proceeding from Int-1. Compound **1u** likely undergoes dealkylation to form **3aa** via an S_N2 mechanism (Table 3B, Pathway I),¹³ which outcompetes reduction and Ni capture. In contrast, bulkier **1x** is likely resistant to nucleophilic dealkylation and preferentially undergoes reduction by Zn to form Int-2. From Int-2, steric hindrance likely deters efficient radical captured by Ni (Pathway III) and instead funnels to dimerization (Pathway II).

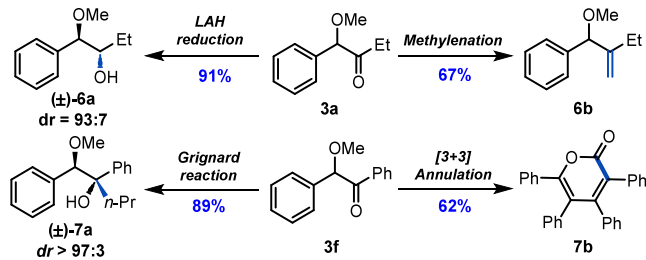
Table 3. Scope of Benzaldehyde Dialkyl and Dibenzyl Acetals^a and Lewis Acid Reactivity Trends



^aIsolated yield from 0.50 mmol using propionic anhydride (2.0 equiv). ^bTMSOTf (2.0 equiv) instead of $\text{BF}_3\text{-OEt}_2$.

Next, to showcase the synthetic utility, α -substituted ethers were transformed into various products displaying useful functionalities (Scheme 2). Compound 3a was reduced with

Scheme 2. Synthetic Derivatizations

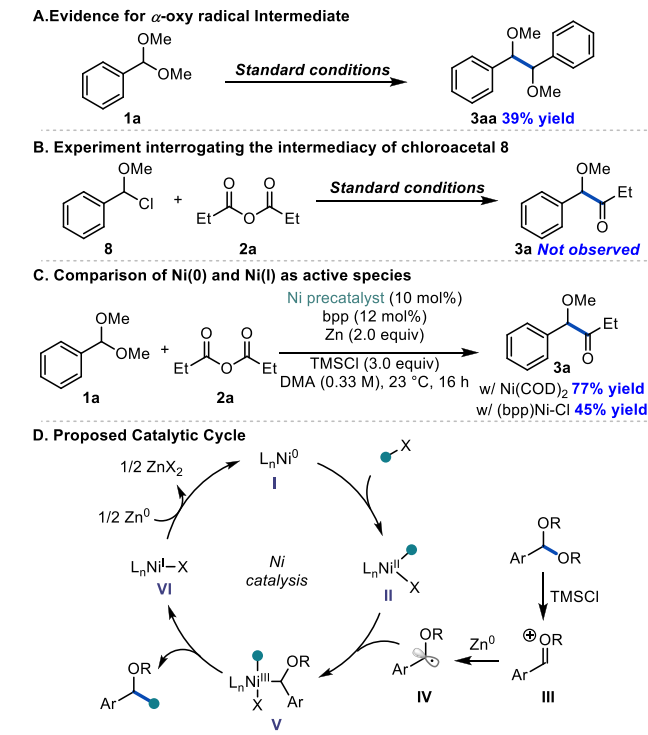


lithium aluminum hydride, yielding the 2° alcohol **6a** in high yield and diastereoselectivity.¹⁴ Methylation of **3a** with bis(iodozincio)methane afforded the alkene **6b**.¹⁵ Grignard addition to **3f** furnished **7a** in excellent yield and diastereoselectivity.¹⁶ Furthermore, **3f** underwent a [3 + 3] annulation reaction to form pyrone **7b**,¹⁷ a pharmacologically relevant structural motif.¹⁸ Furthermore, we demonstrated the practicality of the reaction on a gram scale, which proceeded without loss in yield (91%) (See SI VI-A).

To gain insight into the mechanism, we first sought evidence for the involvement of an α -oxy radical: in the absence of coupling partners, dimer **3aa** formed in 39% yield with 1:1 *dr*

(Scheme 3A).^{5b} A control experiment without the Ni catalyst and bpp ligand afforded **3aa** in 20% yield, suggesting that

Scheme 3. Mechanistic Studies and Proposed Catalytic Cycle



radical formation is possible without Ni complex (see SI VII-A). Furthermore, although TMSCl could generate chloroether **8** as a potential electrophile,^{5c} no product was observed upon subjecting **8** to standard conditions, ruling out this pathway (Scheme 3B). We also sought to identify the active Ni species. Specifically, we aimed to distinguish between two possibilities (see SI Figure S14). In Path a, oxidative addition of anhydride to Ni(0) generates Ni(II),¹⁹ followed by radical capture to afford Ni(III). Reductive elimination yields Ni(I)(X), which reenters the catalytic cycle or is reduced by Zn to generate Ni(0). In Path b, oxidative addition occurs with Ni(I)X to give Ni(III), which undergoes comproportionation with another Ni(I)X to afford Ni(II)RX and Ni(II)X₂.²⁰ The Ni(II)RX captures the α -oxy radical to generate Ni(III), which undergoes reductive elimination to form **3** and Ni(I)X, completing the cycle.

To verify this, we subjected Ni(I)(bpp)Cl, a plausible intermediate for both pathways, to the reaction, which gave a 45% yield (Scheme 3C). However, the use of Ni(0)(COD)₂ gave the product in a 77% yield, suggesting that Path a may be operative. To further probe this pathway and the involvement of Ni(0) as the active species, we examined whether Ni(I)(bpp)Cl could be reduced to Ni(0) in the presence of Zn, analogous to the protocol reported by Weix group with Mn (see SI VII-C-3).²¹ UV-vis analysis showed that Zn reduces Ni(I), evidenced by the disappearance of the 600 nm peak. The spectrum matched that of independently prepared bppNi(0), suggesting that Ni(0) is the active species.

Based on our mechanistic studies and literature precedent, we propose the following mechanism (Scheme 3D).^{5b,19,22} Ni(0) I undergoes oxidative addition with anhydride or vinyl

triflate, generating Ni(II) **II**.²³ The α -oxy radical **IV**, generated from benzaldehyde dialkyl acetal via TMSCl activation to the oxocarbenium ion and Zn reduction, is captured by Ni(II) **II** to form Ni(III) **V**. Reductive elimination then releases the product and generates Ni(I) **VI**, which is subsequently reduced by Zn to Ni(0) **I**. While our data and literature precedent support this Ni(0) cycle, the involvement of a Ni(I) species as the propagating catalyst cannot be completely ruled out.²⁴

In summary, we report a Ni-catalyzed reductive cross-coupling of benzylic acetals with anhydrides or vinyl triflates to access α -substituted ethers. Reactivity was governed by the steric and coordination effects of the Lewis acid. The resulting ethers are readily diversified, and mechanistic studies support Ni(0) as an active species. Further expansion of the C–O bond activation is ongoing.

■ ASSOCIATED CONTENT

Data Availability Statement

The data underlying this study are available in the published article and its [Supporting Information](#).

SI Supporting Information

The Supporting Information is available free of charge at <https://pubs.acs.org/doi/10.1021/acs.orglett.5c02788>.

Experimental details, characterization data, spectroscopic data, and X-ray crystal structure ([PDF](#))

Accession Codes

Deposition Number [2471184](#) contains the supplementary crystallographic data for this paper. These data can be obtained free of charge via the joint Cambridge Crystallographic Data Centre (CCDC) and Fachinformationszentrum Karlsruhe [Access Structures](#) service.

■ AUTHOR INFORMATION

Corresponding Authors

Abigail G. Doyle – Department of Chemistry and Biochemistry, University of California, Los Angeles, California 90095, United States;  [orcid.org/0000-0002-6641-0833](#); Email: agdoyle@chem.ucla.edu

Sun Dongbang – Department of Chemistry, Sogang University, Seoul 04107, Republic of Korea;  [orcid.org/0000-0001-6599-3603](#); Email: dongbang@sogang.ac.kr

Authors

Eunbi Kim – Department of Chemistry, Sogang University, Seoul 04107, Republic of Korea

Meredith A. Borden – Department of Chemistry, Princeton University, Princeton, New Jersey 08544, United States;  [orcid.org/0000-0001-5369-8199](#)

Junha Hwang – Department of Chemistry, Sogang University, Seoul 04107, Republic of Korea

Complete contact information is available at:

<https://pubs.acs.org/10.1021/acs.orglett.5c02788>

Author Contributions

¹E.K. and M.A.B. contributed equally. The manuscript was written through contributions of all authors. All authors have given approval to the final version of the manuscript.

Notes

The authors declare no competing financial interest.

■ ACKNOWLEDGMENTS

This research has been supported by Global - Learning & Academic research institution for Master's-PhD students, and Postdocs(LAMP) Program of the National Research Foundation of Korea(NRF) grant funded by the Ministry of Education (RS-2024-00441954) and National Research Foundation of Korea(NRF) grant funded by the Korea government(MSIT) (RS-2024-00336970). A.G.D. acknowledges generous support from NIH R35 GM-126986. We are grateful to Jihyun Lee (Sogang university) for assistance with the X-ray diffraction data and Prof. Young Hyun Hong (Sogang university) for helpful discussions.

■ REFERENCES

- (1) (a) Tian, Q.; Zhang, G. Recent Advances in the Asymmetric Nozaki-Hiyama-Kishi Reaction. *Synthesis* **2016**, *48*, 4038–4049. (b) Okude, Y.; Hirano, S.; Hiyama, T.; Nozaki, H. Grignard-type Carbonyl Addition of Allyl Halides by Means of Chromous Salt. A Chemospecific Synthesis of Homoallyl Alcohols. *J. Am. Chem. Soc.* **1977**, *99*, 3179–3181. (c) Gil, A.; Albericio, F.; Alvarez, M. Role of the Nozaki-Hiyama-Takai-Kishi Reaction in the Synthesis of Natural Products. *Chem. Rev.* **2017**, *117*, 8420–8446.
- (2) (a) Gaggero, N.; Pandini, S. Advances in Chemoselective Intermolecular Cross-Benzoin-Type Condensation Reactions. *Org. Biomol. Chem.* **2017**, *15*, 6867–6887. (b) Sundermeier, M.; Zapf, A.; Beller, M. Palladium-Catalyzed Cyanation of Aryl Halides: Recent Developments and Perspectives. *Eur. J. Inorg. Chem.* **2003**, *2003*, 3513–3526.
- (3) Molander, G. A.; St. Jean, D. J.; Haas, J. Toward a General Route to the Eunicellin Diterpenes: The Asymmetric Total Synthesis of Deacetoxyalcyonin Acetate. *J. Am. Chem. Soc.* **2004**, *126*, 1642–1643.
- (4) (a) Roughley, S. D.; Jordan, A. M. The Medicinal Chemist's Toolbox: An Analysis of Reactions Used in the Pursuit of Drug Candidates. *J. Med. Chem.* **2011**, *54*, 3451–3479. (b) Ameen, D.; Snape, T. J. Chiral 1,1-Diaryl Compounds as Important Pharmacophores. *Med. Chem. Comm.* **2013**, *4*, 893–907.
- (5) (a) Hatano, B.; Nagahashi, K.; Habaue, S. Reductive Coupling of Aromatic Dialkyl Acetals Using the Combination of Zinc and Chlorotrimethylsilane in the Presence of Potassium Carbonate. *Chem. Lett.* **2007**, *36*, 1418–1419. (b) Arendt, K. M.; Doyle, A. G. Dialkyl Ether Formation by Nickel-Catalyzed Cross-Coupling of Acetals and Aryl Iodides. *Angew. Chem., Int. Ed.* **2015**, *127*, 10014–10018. (c) Lin, Z.; Lan, Y.; Wang, C. Synthesis of Gem-Difluoroalkenes via Nickel-Catalyzed Reductive C–F and C–O Bond Cleavage. *ACS Catal.* **2019**, *9*, 775–780. (d) Rossolini, T.; Ferko, B.; Dixon, D. J. Photocatalytic Reductive Formation of α -Tertiary Ethers from Ketals. *Org. Lett.* **2019**, *21*, 6668–6673.
- (6) Kim, E.; Borden, M. A.; Hwang, J.; Doyle, A. G.; Dongbang, S. Ni-Catalyzed Reductive Coupling of Acetals with Anhydrides and Vinyl Triflates via Single-Electron C–O Activation: A Polarity-Convergent Approach to Native and Umpolung Aldehyde Reactivity. *ChemRxiv* **2025**, DOI: [10.26434/chemrxiv-2025-twntt](https://doi.org/10.26434/chemrxiv-2025-twntt).
- (7) (a) Kariofillis, S. K.; Shields, B. J.; Tekle-Smith, M. A.; Zacuto, M. J.; Doyle, A. G. Nickel/Photoredox-Catalyzed Methylation of (Hetero)aryl Chlorides Using Trimethyl Orthoformate as a Methyl Radical Source. *J. Am. Chem. Soc.* **2020**, *142*, 7683–7689. (b) Kariofillis, S. K.; Jiang, S.; Źurański, A. M.; Gandhi, S. S.; Martinez Alvarado, J. I.; Doyle, A. G. Using Data Science To Guide Aryl Bromide Substrate Scope Analysis in a Ni/Photoredox-Catalyzed Cross-Coupling with Acetals as Alcohol-Derived Radical Sources. *J. Am. Chem. Soc.* **2022**, *144*, 1045–1055. (c) Romano, C.; Talavera, L.; Gómez-Bengoa, E.; Martin, R. Conformational Flexibility as a Tool for Enabling Site-Selective Functionalization of Unactivated sp^3 C–O Bonds in Cyclic Acetals. *J. Am. Chem. Soc.* **2022**, *144*, 11558–11563. (d) Dongbang, S.; Doyle, A. G. Ni/Photoredox-Catalyzed C(sp^3)–C(sp^3) Coupling between Aziridines and Acetals as Alcohol-Derived Alkyl Radical Precursors. *J. Am. Chem. Soc.* **2022**, *144*, 20067–20077.

(8) Langdon, S. M.; Wilde, M. M. D.; Thai, K.; Gravel, M. Chemoselective *N*-Heterocyclic Carbene-Catalyzed Cross-Benzoin Reactions: Importance of the Fused Ring in Triazolium Salts. *J. Am. Chem. Soc.* **2014**, *136*, 7539–7542.

(9) Classical NHK reactions use stoichiometric chromium, but recent advances enable catalytic variants. For examples, see: (a) Fürstner, A.; Shi, N. A Multicomponent Redox System Accounts for the First Nozaki–Hiyama–Kishi Reactions Catalytic in Chromium. *J. Am. Chem. Soc.* **1996**, *118*, 2533–2534. (b) Calogero, F.; Potenti, S.; Magagnano, G.; Mosca, G.; Gualandi, A.; Marchini, M.; Ceroni, P.; Cozzi, P. G. A Photoredox Nozaki–Hiyama Reaction Catalytic in Chromium. *Eur. J. Org. Chem.* **2022**, *2022*, e202200350. (c) Gao, Y.; Jiang, B.; Friede, N. C.; Hunter, A. C.; Boucher, D. G.; Minteer, S. D.; Sigman, M. S.; Reisman, S. E.; Baran, P. S. Electrocatalytic Asymmetric Nozaki–Hiyama–Kishi Decarboxylative Coupling: Scope, Applications, and Mechanism. *J. Am. Chem. Soc.* **2024**, *146*, 4872–4882.

(10) Joe, C. L.; Doyle, A. G. Direct Acylation of $C(sp^3)$ –H Bonds Enabled by Nickel and Photoredox Catalysis. *Angew. Chem., Int. Ed.* **2016**, *128*, 4108–4111.

(11) See **SI** for the details about **3q**. Chemical equilibrium of intermediate for **3q**:

3q

(12) Shamsuzzaman; Dar, A. M.; Khanam, H.; Gato, M. A. Anticancer and Antimicrobial Evaluation of Newly Synthesized Steroidal 5,6 Fused Benzothiazines. *Arab. J. Chem.* **2014**, *7*, 461–468.

(13) Node, M.; Nishide, K.; Sai, M.; Fujita, E. Dealkylation of esters and cleavage of alcoholic carbon–oxygen bond of lactones with aluminium halide–thiol system. *Tetrahedron Lett.* **1978**, *19*, 5211–5214.

(14) The relative configuration of **6a** was confirmed by X-ray diffraction analysis using an acylated derivative of **6a** (see **SI VI-B-2**). CCDC 2471184 data of acylated derivative of **6a** can be obtained free of charge from The Cambridge Crystallographic Data Center.

(15) Sada, M.; Komagawa, S.; Uchiyama, M.; Kobata, M.; Mizuno, T.; Utimoto, K.; Oshima, K.; Matsubara, S. Reaction Pathway of Methylenation of Carbonyl Compounds with Bis(Iodozincio)–Methane. *J. Am. Chem. Soc.* **2010**, *132*, 17452–17458.

(16) Read, J. A.; Yang, Y.; Woerpel, K. A. Additions of Organomagnesium Halides to α -Alkoxy Ketones: Revision of the Chelation-Control Model. *Org. Lett.* **2017**, *19*, 3346–3349.

(17) (a) McGlacken, G. P.; Fairlamb, I. J. S. 2-Pyrone Natural Products and Mimetics: Isolation, Characterisation and Biological Activity. *Nat. Prod. Rep.* **2005**, *22*, 369–385. (b) Goel, A.; Ram, V. J. Natural and Synthetic 2H-Pyran-2-Ones and Their Versatility in Organic Synthesis. *Tetrahedron* **2009**, *65*, 7865–7913.

(18) Bai, D.; Chen, J.; Zheng, B.; Li, X.; Chang, J. Catalytic [3 + 3] Annulation of β -Ketoethers and Cyclopropenones via $C(sp^3)$ –O/C–C Bond Cleavage under Transition-Metal Free Conditions. *Chin. J. Chem.* **2021**, *39*, 2769–2773.

(19) Ni, S.; Padial, N. M.; Kingston, C.; Vantourout, J. C.; Schmitt, D. C.; Edwards, J. T.; Kruszyk, M. M.; Merchant, R. R.; Mykhailiuk, P. K.; Sanchez, B. B.; Yang, S.; Perry, M. A.; Gallego, G. M.; Mousseau, J. J.; Collins, M. R.; Cherney, R. J.; Lebed, P. S.; Chen, J. S.; Qin, T.; Baran, P. S. A Radical Approach to Anionic Chemistry: Synthesis of Ketones, Alcohols, and Amines. *J. Am. Chem. Soc.* **2019**, *141*, 6726–6739.

(20) (a) Cagan, D. A.; Bím, D.; McNicholas, B. J.; Kazmierczak, N. P.; Oyala, P. H.; Hadt, R. G. Photogenerated Ni(I)–Bipyridine Halide Complexes: Structure–Function Relationships for Competitive $C(sp^2)$ –Cl Oxidative Addition and Dimerization Reactivity Pathways. *Inorg. Chem.* **2023**, *62*, 9538–9551. (b) Ting, S. I.; Williams, W. L.; Doyle, A. G. Oxidative Addition of Aryl Halides to a Ni(I)–Bipyridine Complex. *J. Am. Chem. Soc.* **2022**, *144*, 5575–5582.

(21) (a) Su, Z.-M.; Deng, R.; Stahl, S. S. Zinc and Manganese Redox Potentials in Organic Solvents and Their Influence on Nickel-Catalyzed Cross-Electrophile Coupling. *Nat. Chem.* **2024**, *16*, 2036–2043. (b) Huang, Z.; Akana, M. E.; Sanders, K. M.; Weix, D. J. A Decarbonylative Approach to Alkylnickel Intermediates and $C(sp^3)$ – $C(sp^3)$ Bond Formation. *Science* **2024**, *385*, 1331–1337.

(22) Gutierrez, O.; Tellis, J. C.; Primer, D. N.; Molander, G. A.; Kozlowski, M. C. Nickel-Catalyzed Cross-Coupling of Photoredox-Generated Radicals: Uncovering a General Manifold for Stereoconvergence in Nickel-Catalyzed Cross-Couplings. *J. Am. Chem. Soc.* **2015**, *137*, 4896–4899.

(23) (a) Shu, X.; Huan, L.; Huang, Q.; Huo, H. Direct Enantioselective $C(sp^3)$ –H Acylation for the Synthesis of α -Amino Ketones. *J. Am. Chem. Soc.* **2020**, *142*, 19058–19064. (b) Li, T.; Luo, L.; Cheng, X.; Lu, Z. Enantioconvergent Cross-Coupling Reaction with 1,4-Dihydropyridine Derivatives via Photoinduced Nickel Catalysis. *ACS. Catal.* **2024**, *14*, 3278–3286.

(24) An alternative pathway cannot be excluded, wherein the α -oxy radical first adds to Ni(0) I to afford a Ni(I) intermediate, which then undergoes oxidative addition with the anhydride (see **SI S18**). Yet, given the nucleophilic nature of the α -oxy radical, it is more likely to add to the more electron-deficient Ni(II) rather than the electron-rich Ni(0). Moreover, since Ni(II) is likely the resting state, its higher steady-state concentration would increase the likelihood of radical capture. We therefore consider this scenario less likely. (a) Lyon, W. L.; MacMillan, D. W. C. Expedient Access to Underexplored Chemical Space: Deoxygenative $C(sp^3)$ – $C(sp^3)$ Cross-Coupling. *J. Am. Chem. Soc.* **2023**, *145*, 7736–7742. (b) Wang, H.; Liu, C. F.; Song, Z.; Yuan, M.; Ho, Y. A.; Gutierrez, O.; Koh, M. J. Engaging α -Fluorocarboxylic Acids Directly in Decarboxylative C–C Bond Formation. *ACS. Catal.* **2020**, *10*, 4451–4459. For examples of nucleophilic radical additions to electron-deficient alkenes, see: (c) Yang, T.; Xiong, W.; Sun, G.; Yang, W.; Lu, M.; Koh, M. J. Multicomponent Construction of Tertiary Alkylamines by Photoredox/Nickel-Catalyzed Aminoalkylation of Organohalides. *J. Am. Chem. Soc.* **2024**, *146*, 29177–29188. (d) Garwood, J. J. A.; Chen, A. D.; Nagib, D. A. Radical Polarity. *J. Am. Chem. Soc.* **2024**, *146*, 28034–28059. For example of where Ni(II) is the resting state, see: (e) Cusumano, A. Q.; Chaffin, B. C.; Doyle, A. G. Mechanism of Ni-Catalyzed Photochemical Halogen Atom-Mediated $C(sp^3)$ –H Arylation. *J. Am. Chem. Soc.* **2024**, *146*, 15331–1534.